Langmuir

Letter

pubs.acs.org/Langmuir

Magnetic-Field-Assisted Fabrication and Manipulation of Nonspherical Polymer Particles in Ferrofluid-Based Droplet Microfluidics

Taotao Zhu,[†] Rui Cheng,[‡] Gareth R. Sheppard,[†] Jason Locklin,[†] and Leidong Mao*[,‡]

[†]Department of Chemistry and [‡]College of Engineering, University of Georgia, Athens, Georgia 30602, United States

ABSTRACT: We report a novel magnetic-field-assisted method for the fabrication and manipulation of nonspherical polymer particles within a ferrofluid-based droplet microfluidic device. Shape control and chain assembly of droplets with tunable lengths have been achieved.

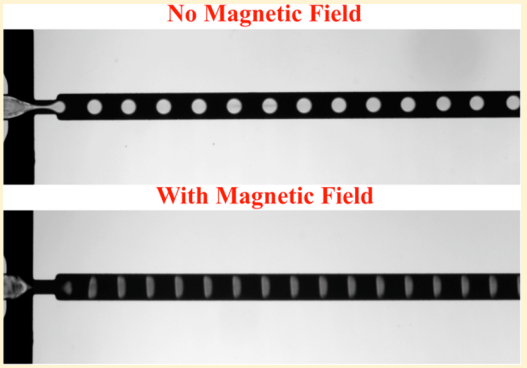

(1). INTRODUCTION

Functional polymer particles with uniform sizes and shapes have been proven useful in a wide variety of applications including cosmetics, biotechnology, and pharmaceuticals.[1−4] Traditionally, the dominant shape of polymer particles has been spherical because of their manufacturing technique, which typically involves emulsion and suspension polymerization. The surface tension between the polymer solution and the surrounding medium naturally favors surface area minimization, leading to spherical particles.[5] Nonspherical particles, on the other hand, are beneficial to many applications including drug delivery, bioimaging, and biomimetics due to their large surface area and anisotropic responses to external hydrodynamic, electrical, and magnetic stimulation.[6−10] The particle chain structure with tunable length produced by this technique can potentially be applied in microswimmer and surface topography.[11,12] Strategies to fabricate nonspherical polymer particles include template-assisted polymerization and controlled polymer nucleation and growth.[13] However, it remains difficult to fabricate large quantities of monodisperse particles with tunable shapes and sizes.[5]

Recently, flow lithography was developed to form two-dimensional and three-dimensional nonspherical particles of the desired shapes within a microfluidic device through combining mask-based lithography and photopolymerization.[14−18] At the same time, droplet microfluidics also presents an alternative strategy for the generation of monodisperse polymer droplets by coflowing a polymer phase and an immiscible continuous phase together within a microfluidic device.[19−21] On one hand, the sizes of droplets can be controlled via the ratio of the flow rates of two phases. A downstream ultraviolet (UV) light source can solidify the droplets carrying UV-curable polymer rapidly to preserve their shapes. Using the size of the microchannel as confinement, particles with disk, plug, and rod shapes have been successfully fabricated.[13] On the other hand, the functionalities of particles can be designed, added, and controlled by the magnetic[22−25] responses of polymer blends in the droplet.

In this study, we present a new method that can control the shape and assembly of polymer droplets within a flow-focusing droplet microfluidic device to form nonspherical particles and chains. This method, relying on a water-based magnetic liquid (ferrofluid) as a continuous phase to (1) induce droplet formation, (2) controllably change the shape of droplets, and (3) assemble droplets into chains, is based on the magnetic buoyancy force and dipole−dipole interactions in the ferrofluids. The manipulation of droplets within ferrofluids occurs under external magnetic fields. Ferrofluids are stable colloidal suspensions of magnetic nanoparticles. The purpose of using ferrofluids is to induce an effective magnetic dipole moment within the droplets immersed in ferrofluids. The droplets, experiencing a large magnetic field, can both deform to nonspherical shapes and assemble into chains of tunable lengths.

(2). EXPERIMENTAL SECTION

Schematics and a prototype ferrofluid-based droplet microfluidic device are shown in Figure 1A,B. The polymer phase (monomer mixed with photoinitiator) was introduced into the microfluidic channel (inlet 2 in Figure 1A) and hydrodynamically focused by ferrofluid sheath flow (inlet 1 in Figure 1A). Droplets were induced when proper flow rates of the polymer phase and ferrofluid continuous

Received: June 9, 2015
Revised: July 22, 2015
Published: July 27, 2015

DOI: 10.1021/acs.langmuir.5b02097
Langmuir 2015, 31, 8531−8534

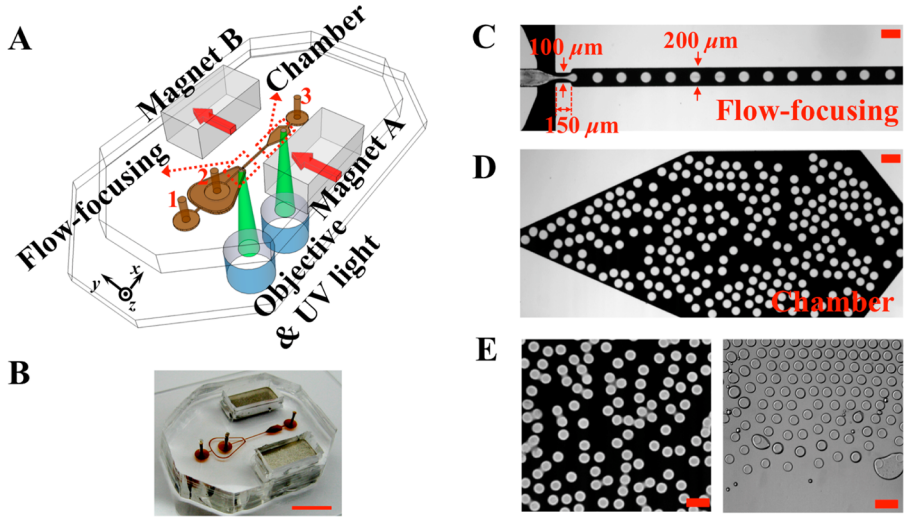

Figure 1. (A) Schematic representation of the ferrofluid-based droplet microfluidic device. Arrows in magnets indicate the directions of magnetization. The magnetic flux density in the channel is estimated to be ~500 mT. (B) Prototype device; the scale bar is 10 mm. Generation (C, flow-focusing area; D, chamber area) and polymerization (E, left, with ferrofluids; E, right, without ferrofluids) of droplets within the device. Scale bars in C–E are 200 μm.

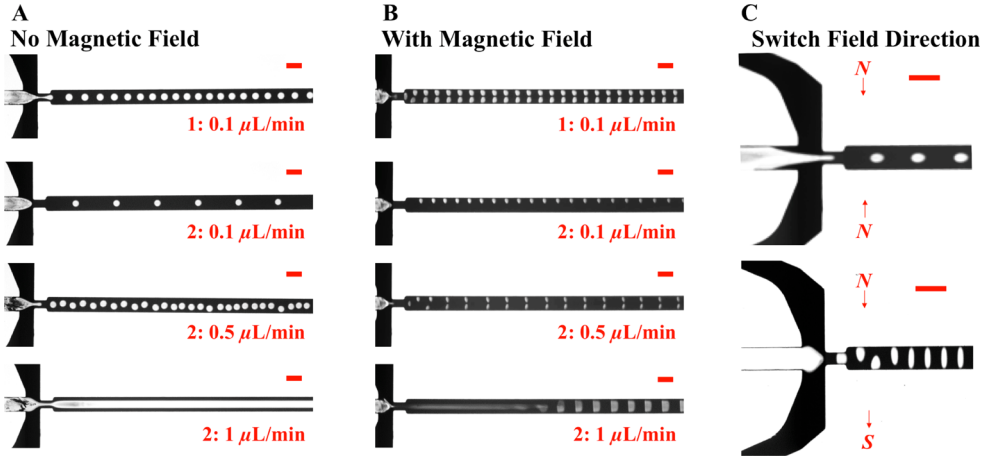

Figure 2. (A) Spherical polymer droplet generation with no magnetic field. The sizes of the droplets can be controlled by adjusting the flow rate ratio between the polymer phase and the continuous ferrofluid phase. (B) Nonspherical polymer droplet generation with magnetic fields induced by attractively placed magnets. (C) Polymer droplets are either compressed or stretched into an ellipsoidal shape by arranging magnets differently (in an attractive manner or in a repulsive manner, as indicated by the arrows). Scale bars in A–C are 200 μm.

phase were reached, as demonstrated in Figure 1C,D. UV exposure in the chamber photopolymerized droplets into solids (Figure 1E). Magnets A and B indicated in Figures 1A were used to control the shapes and assembly of droplets.

The continuous phase is a commercial water-based magnetite ferrofluid (EMG 705, Ferrotec Co., Bedford, NH). The volume fraction of the magnetite particles for this particular ferrofluid is 5.8%. The mean diameter of nanoparticles has been determined from transmission electron microscopy (TEM) images to be 10.2 nm. The initial magnetic susceptibility is 1.17, the saturation magnetization (μ_0M) is 325 G, and the viscosity is 4.5×10^{-3} kg/m·s. The ferrofluid was mixed with 0.1% Tween 20 (5% w/w) to prevent droplet coalescence. The polymer phase consists of monomer (polypropylene glycol diacrylate) and photoinitiator (hydroxycyclohexyl phenyl ketone, 6% w/w), with an estimated viscosity of 6.8×10^{-2} kg/m·s.

The PDMS microfluidic channel was fabricated through a standard soft-lithograph approach and attached to the flat surface of another piece of PDMS. Dimensions of the microfluidic channel are listed in Figure 1. The thickness of the channel was measured to be 44 μm by a profilometer (Dektak 150, Veeco Instruments Inc., Chadds Ford, PA). Experiments were conducted on the stage of an inverted microscope (Zeiss Axio Observer, Carl Zeiss Inc., Germany). During experiments, ferrofluid and polymer injections into microchannel were maintained at variable flow rates using syringe pumps (Nexus 3000, Chemyx Inc., Stafford, TX). Two NdFeB permanent magnets were used to produce the required magnetic fields for shape control and assembly of droplets. Each magnet is 6.4 mm in width, 12.7 mm in length, and 5 mm in thickness. The magnetic flux density at the center of the magnets' pole surface was measured to be 0.36 T by a Gauss meter (model 5080, Sypris, Orlando, FL) and an axial probe with a 0.381 mm diameter of circular active area. The images of droplets were recorded using a CCD camera (SPOT RT3, Diagnostic Instruments, Inc., Sterling Heights, MI). A 120 W xenon lamp (X-cite 120Q, Lumen Dynamics Inc., Ontario, Canada) served as a UV exposure source. The desired wavelength of UV light for photopolymerization was selected using a UV filter set (11000 v3, Chroma Technology Corp., Rockingham, VT). Areas of polymerization were controlled via a 20× objective and the built-in aperture of the inverted microscope.

DOI: 10.1021/acs.langmuir.5b02097
Langmuir 2015, 31, 8531–8534

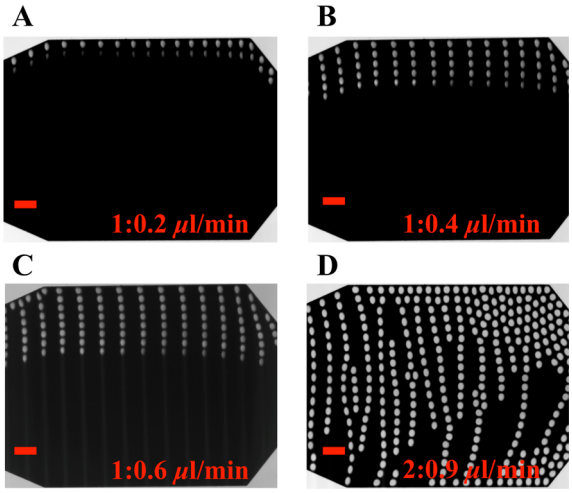

Figure 3. Chain formation of polymer droplets under the same magnetic fields. (A) Length of chain, 2. (B) Length of chain, 5. (C) Length of chain, 8. (D) Long chains forming at a higher polymer phase flow rate. Scale bars in A–D are 400 μm.

(3). RESULTS AND DISCUSSION

(3.1) Droplet Shape Control. When an external magnetic field gradient is applied, nonmagnetic droplets inside ferrofluids experience both magnetic and hydrodynamic drag forces, $\mathbf{F}_m$ and $\mathbf{F}_d$. In the cases of diluted ferrofluids or an intense applied magnetic field, the magnetic buoyancy force on a nonmagnetic droplet inside ferrofluids can be expressed as[26] $\mathbf{F}_m = -V\mu_0(\mathbf{M}\cdot\nabla)\mathbf{H}$, where V is the volume of the droplet (~50 μm in diameter and ~40 μm in thickness, disk shape) and μ_0 is the permeability of free space. $\mathbf{M}$ is the effective magnetization of the ferrofluid (~5×10^3 A/m), and $\mathbf{H}$ is the applied magnetic field (~4×10^5 A/m). The gradient of the magnetic field is ~2×10^7 A/m^2. The presence of the minus sign in front of the term indicates that the nonmagnetic particle immersed in ferrofluids experiences a force in the direction of the weaker magnetic field. The estimated magnetic force on each droplet is on the order of 10 nN, which is much larger than the viscous drag force. This force can be used to stretch the spherical shape of droplets into ellipsoids of different sizes, as shown in Figure 2. Other shapes are also possible with different designs of magnetic field patterns. Droplets of larger size experienced more magnetic buoyancy forces than smaller ones. This phenomenon can potentially be used to continuously separate droplets inside a ferrofluid based on their sizes.[27−30]

(3.2) Droplet Assembly. Nonmagnetic droplets in the chamber area immersed in ferrofluids behave like "magnetic holes" and exhibit characteristics of magnetic dipoles. These droplets experiences dipole−dipole interactions, leading to the assembly of linear chains with tunable lengths oriented along the magnetic field $\mathbf{H}$ direction (y direction in Figure 1A). The magnetic energy between droplets depends on the volume of droplets, the susceptibility of the ferrofluids, and the strength of the magnetic field. In this study, the maximum magnetic energy is estimated to be ~5×10^{-10} J, much larger than the thermal fluctuation energy, kT, making the assembly of droplets in ferrofluids extremely efficient. Figure 3 depicts the droplets chain formation with variable lengths in the chamber.

(3.3) Droplet Chain Photopolymerization. Nonspherical droplets were photopolymerized in the chamber under magnetic fields. Microscopic and SEM images in Figure 4 confirmed that the particles were able to retain their shapes and chains after solidification.

(4). CONCLUSIONS AND OUTLOOK

We developed a novel method for the fabrication and manipulation of polymer particles within a ferrofluid-based droplet microfluidic device. The shape and assembly of polymer particles could be controlled via the flow rate and external magnetic field. In this study, the ellipsoidal shape and linear chains of particles were demonstrated. Other types of shapes and assemblies are possible with different combinations of flow rates and magnetic field patterns.

AUTHOR INFORMATION

Corresponding Author

* Tel: +1-706-542-1871. Fax: +1-706-542-3804. E-mail: mao@uga.edu.

Present Address

(T.Z.) Procter & Gamble, 8256 Union Center Blvd, West Chester, OH 45069, United States.

Notes

The authors declare no competing financial interest.

ACKNOWLEDGMENTS

This material is based upon work supported by the National Science Foundation under grant no. 1150042.

REFERENCES

(1) Nisisako, T.; Torii, T.; Takahashi, T.; Takizawa, Y. Synthesis of monodisperse bicolored janus particles with electrical anisotropy using a microfluidic co-flow system. *Adv. Mater.* **2006**, *18* (9), 1152−1156.

(2) Murray, M. J.; Snowden, M. J. The preparation, characterisation and applications of colloidal microgels. *Adv. Colloid Interface Sci.* **1995**, *54*, 73−91.

(3) Yoshida, M.; Roh, K. H.; Lahann, J. Short-term biocompatibility of biphasic nanocolloids with potential use as anisotropic imaging probes. *Biomaterials* **2007**, *28* (15), 2446−2456.

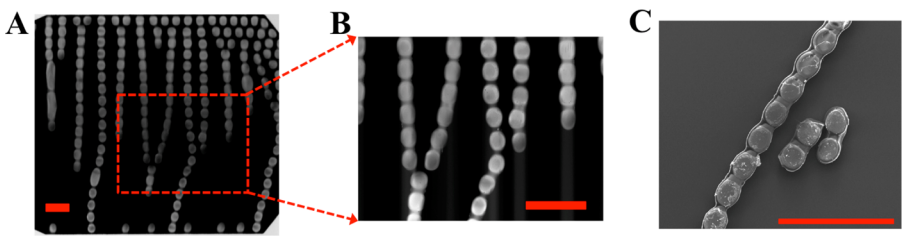

Figure 4. Photopolymerization of droplet chains under magnetic fields. (A, B). Microscopic images of solidified droplets after UV exposure. (C). SEM image of solidified droplet chain. Scale bars in A–C are 400 μm.

DOI: 10.1021/acs.langmuir.5b02097
Langmuir 2015, 31, 8531−8534

(4) Pankhurst, Q. A.; Connolly, J.; Jones, S. K.; Dobson, J. Applications of magnetic nanoparticles in biomedicine. *J. Phys. D: Appl. Phys.* **2003**, *36* (13), R167−R181.
(5) Shum, H. C.; Abate, A. R.; Lee, D.; Studart, A. R.; Wang, B.; Chen, C.-H.; Thiele, J.; Shah, R. K.; Krummel, A.; Weitz, D. A. Droplet Microfluidics for Fabrication of Non-Spherical Particles. *Macromol. Rapid Commun.* **2010**, *31* (2), 108−118.
(6) Allen, T. M.; Cullis, P. R. Drug delivery systems: Entering the mainstream. *Science* **2004**, *303* (5665), 1818−1822.
(7) Walther, A.; Muller, A. H. E. Janus particles. *Soft Matter* **2008**, *4* (4), 663−668.
(8) Whitehead, K. A.; Colligon, J.; Verran, J. Retention of microbial cells in substratum surface features of micrometer and sub-micrometer dimensions. *Colloids Surf., B* **2005**, *41* (2−3), 129−138.
(9) Champion, J. A.; Katare, Y. K.; Mitragotri, S. Making polymeric micro- and nanoparticles of complex shapes. *Proc. Natl. Acad. Sci. U. S. A.* **2007**, *104* (29), 11901−11904.
(10) Mathaes, R.; Winter, G.; Besheer, A.; Engert, J. Non-spherical micro- and nanoparticles: fabrication, characterization and drug delivery applications. *Expert Opin. Drug Delivery* **2015**, *12* (3), 481−492.
(11) Biswal, S. L.; Gast, A. P. Rotational dynamics of semiflexible paramagnetic particle chains. *Phys. Rev. E* **2004**, *69*, 4.
(12) Luong-Van, E.; Rodriguez, I.; Low, H. Y.; Elmouelhi, N.; Lowenhaupt, B.; Natarajan, S.; Lim, C. T.; Prajapati, R.; Vyakarnam, M.; Cooper, K. Review: Micro- and nanostructured surface engineering for biomedical applications. *J. Mater. Res.* **2013**, *28* (2), 165−174.
(13) Hwang, D. K.; Dendukuri, D.; Doyle, P. S. Microfluidic-based synthesis of non-spherical magnetic hydrogel microparticles. *Lab Chip* **2008**, *8* (10), 1640−1647.
(14) Dendukuri, D.; Pregibon, D. C.; Collins, J.; Hatton, T. A.; Doyle, P. S. Continuous-flow lithography for high-throughput microparticle synthesis. *Nat. Mater.* **2006**, *5* (5), 365−369.
(15) Dendukuri, D.; Gu, S. S.; Pregibon, D. C.; Hatton, T. A.; Doyle, P. S. Stop-flow lithography in a microfluidic device. *Lab Chip* **2007**, *7* (7), 818−828.
(16) Jang, J. H.; Dendukuri, D.; Hatton, T. A.; Thomas, E. L.; Doyle, P. S. A route to three-dimensional structures in a microfluidic device: Stop-flow interference lithography. *Angew. Chem., Int. Ed.* **2007**, *46* (47), 9027−9031.
(17) Shepherd, R. F.; Panda, P.; Bao, Z.; Sandhage, K. H.; Hatton, T. A.; Lewis, J. A.; Doyle, P. S. Stop-Flow Lithography of Colloidal, Glass, and Silicon Microcomponents. *Adv. Mater.* **2008**, *20* (24), 4734.
(18) Hwang, D. K.; Oakey, J.; Toner, M.; Arthur, J. A.; Anseth, K. S.; Lee, S.; Zeiger, A.; Van Vliet, K. J.; Doyle, P. S. Stop-Flow Lithography for the Production of Shape-Evolving Degradable Microgel Particles. *J. Am. Chem. Soc.* **2009**, *131* (12), 4499−4504.
(19) Xu, S. Q.; Nie, Z. H.; Seo, M.; Lewis, P.; Kumacheva, E.; Stone, H. A.; Garstecki, P.; Weibel, D. B.; Gitlin, I.; Whitesides, G. M. Generation of monodisperse particles by using microfluidics: Control over size, shape, and composition. *Angew. Chem., Int. Ed.* **2005**, *44* (5), 724−728.
(20) Thorsen, T.; Roberts, R. W.; Arnold, F. H.; Quake, S. R. Dynamic pattern formation in a vesicle-generating microfluidic device. *Phys. Rev. Lett.* **2001**, *86* (18), 4163−4166.
(21) Wang, J. T.; Wang, J.; Han, J. J. Fabrication of Advanced Particles and Particle-Based Materials Assisted by Droplet-Based Microfluidics. *Small* **2011**, *7* (13), 1728−1754.
(22) Jeong, J.; Um, E.; Park, J. K.; Kim, M. W. One-step preparation of magnetic Janus particles using controlled phase separation of polymer blends and nanoparticles. *RSC Adv.* **2013**, *3* (29), 11801−11806.
(23) Ge, X. H.; Huang, J. P.; Xu, J. H.; Luo, G. S. Controlled stimulation-burst targeted release by smart decentered core-shell microcapsules in gravity and magnetic field. *Lab Chip* **2014**, *14* (23), 4451−4454.
(24) Chen, Y. H.; Nurumbetov, G.; Chen, R.; Ballard, N.; Bon, S. A. F. Multicompartmental Janus Microbeads from Branched Polymers by Single-Emulsion Droplet Microfluidics. *Langmuir* **2013**, *29* (41), 12657−12662.
(25) Xu, K.; Ge, X. H.; Huang, J. P.; Dang, Z. X.; Xu, J. H.; Luo, G. S. A region-selective modified capillary microfluidic device for fabricating water-oil Janus droplets and hydrophilic-hydrophobic anisotropic microparticles. *RSC Adv.* **2015**, *5* (58), 46981−46988.
(26) Rosensweig, R. E. *Ferrohydrodynamics*; Cambridge University Press: Cambridge, U.K., 1985.
(27) Zhu, T. T.; Marrero, F.; Mao, L. D. Continuous separation of non-magnetic particles inside ferrofluids. *Microfluid. Nanofluid.* **2010**, *9* (4−5), 1003−1009.
(28) Kose, A. R.; Fischer, B.; Mao, L.; Koser, H. Label-free cellular manipulation and sorting via biocompatible ferrofluids. *Proc. Natl. Acad. Sci. U. S. A.* **2009**, *106* (51), 21478−21483.
(29) Zhu, T. T.; Cheng, R.; Lee, S. A.; Rajaraman, E.; Eiteman, M. A.; Querec, T. D.; Unger, E. R.; Mao, L. D. Continuous-flow ferrohydrodynamic sorting of particles and cells in microfluidic devices. *Microfluid. Nanofluid.* **2012**, *13* (4), 645−654.
(30) Zhu, T. T.; Cheng, R.; Liu, Y. F.; He, J.; Mao, L. D. Combining positive and negative magnetophoreses to separate particles of different magnetic properties. *Microfluid. Nanofluid.* **2014**, *17* (6), 973−982.

DOI: 10.1021/acs.langmuir.5b02097
Langmuir 2015, 31, 8531−8534